Solitary Waves in an Inextensible, Flexible, Helicoidal Fiber

Leonid Slepyan, Viacheslav Krylov, and Raymond Parnes
Department of Solid Mechanics, Materials and Structures, Faculty of Engineering, Tel Aviv University, 69978 Tel Aviv, Israel
(Received 31 August 1994)

The exact solution to the nonlinear vector equations governing an inextensible, flexible, helicoidal fiber yields a one-parameter set of solitary waves. Analytical expressions are found for the displacements, internal force, axial and angular momenta, and energy. This solution represents an interesting example of three-dimensional solitary waves propagating in a system devoid of potential energy.

PACS numbers: 62.30.+d, 03.40.Kf

Nonlinear waves in flexible wavy fibers are due to the interaction of longitudinal and transverse oscillations. Such a process has been considered to describe plane [1] and spatial [2–4] motions of a one-dimensional atomic chain (a mass-spring system). Elastic extensional waves in strings were considered in [5–7]. Bending waves were examined in [8,9] for elastic beams and wires under a constant, uniformly distributed tension force. The propagation of solitary waves due to interaction of quantum and mechanical effects was described in [10,11] for the alpha helix as a model of a molecular system.

In the present work, as the simplest system of this kind, we consider a helix consisting of an inextensible fiber with no bending stiffness. Such a system devoid of strain energy is, in its simplicity, comparable to an ideal gas of rigid particles. The helix model is of particular interest since, irrespective of initial helix geometry or amplitude of displacements, a complete and general analytical solution of the nonlinear vector equations governing the dynamics of the fiber is obtained. The solution reveals the existence of three-dimensional solitary waves which possess axial and angular momenta. For a helix of long lead, when the angular momentum is negligible, the shape of the distribution of the force coincides asymptotically with that of solitons governed by the well-known Korteweg–de Vries (KdV) equation.

It may be noted that helicoidal systems are relevant to a wide variety of fields in which coiled structures are important, from the modeling of macromolecules such as DNA to video or audio tapes, storage spool dynamics, and deployable structures for satellite applications [12]. Three-dimensional spatial chaos obtained by numerical simulations in [12] resembles a soliton gas of the waves described below. Moreover, such a system can be used as an energy absorber under dynamic extension [13]. Note that the deployable systems may also serve as demonstrations of the solitary waves.

We consider an inextensible, flexible fiber of mass density ρ per unit length whose equation of motion and extensibility condition are, respectively,

$$[F(S,t)\boldsymbol{\mathcal{R}}'(S,t)]' = \rho\ddot{\boldsymbol{\mathcal{R}}}(S,t), \tag{1a}$$

$$|\boldsymbol{\mathcal{R}}'| = 1. \tag{1b}$$

Here, F is a non-negative tension force, and $\boldsymbol{\mathcal{R}}$ is the position vector. Primes and dots appearing above denote derivatives with respect to the coordinate along the fiber, S, and time, t, respectively.

Our goal is to find a steady-state solution to these equations for a solitary wave in the helix. However, first, the trivial case which corresponds to a fiber of arbitrary shape under a constant tension force, F, deserves to be mentioned. In this case the D'Alembert solution, $\boldsymbol{\mathcal{R}} = \boldsymbol{\mathcal{R}}(S - ct)$, $c = \pm\sqrt{F/\rho}$, where $\boldsymbol{\mathcal{R}}$ is an arbitrary vector function which satisfies the equality (1b), is valid. Since the particle velocity $\partial\boldsymbol{\mathcal{R}}/\partial t$ and the tangent vector $-c\partial\boldsymbol{\mathcal{R}}/\partial S$ coincide, this solution corresponds to a flow of the fiber material along the trajectory defined by the given geometry of the arbitrary fiber, and thus, for this trivial case, the geometry of the fiber remains constant.

We now consider a helix of initial radius R_0 and let γ denote the initial angle between the fiber and the axis of the helix, x. We note that to an observer moving along the helicoidal fiber with a speed v, and the associated angular velocity about the x axis, $v\sin\gamma/R_0$ (with an orthogonal triad natural to the helix), the initial geometry appears invariant; hence a solitary wave is expected to exist as a steady-state solution in a coordinate system attached to the moving observer.

Letting $\boldsymbol{\mathcal{R}}(S,t)$ be represented as the sum of the longitudinal vector, $\mathbf{R}_x(S,t)$, and a vector $\mathbf{R}(S,t)$ lying in the cross section of the helix, we introduce the nondimensional quantities

$$\mathbf{r}_x = \mathbf{R}_x/R_0, \qquad \mathbf{r} = \mathbf{R}/R_0, \qquad s = S/R_0$$
$$f = F/\rho v^2, \qquad \tau = vt/R_0, \tag{2}$$

and express the vectors $\mathbf{r}_x$ and $\mathbf{r}$ as follows:

$$\mathbf{r}_x(s,\xi) = [s\cos\gamma + u(\xi)]\mathbf{k}_x, \qquad \mathbf{r}(s,\xi) = A(\xi)e^{i\lambda s},$$
$$\lambda = \sin\gamma, \qquad \xi = s - \tau, \tag{3}$$

where $A(\xi)$ and $u(\xi)$ are arbitrary functions. For $v > 0$, the conditions at infinity are expected to correspond to the initial shape of the helix, i.e.,

$$(u, u', A', f) \to 0, \qquad A \to 1 \qquad (\xi \to +\infty, \tau \geq 0). \tag{4}$$

0031-9007/95/74(14)/2725(4)$06.00

Here and below, primes and dots denote derivatives with respect to the nondimensional coordinate, s, and time, τ, respectively.

Note that the vector $\mathbf{r}(s,\xi)$ is defined in a complex variable plane which coincides with the cross section of the helix. Substitution in Eq. (1a) then leads to

$$[(\cos\gamma + u')f]' = u'', \tag{5a}$$

$$(1-f)\mathbf{r}'' - f'\mathbf{r}' - \lambda^2\mathbf{r} - 2i\lambda\mathbf{r}' = 0. \tag{5b}$$

Equation (5a) yields immediately an expression for u', namely,

$$u' = \frac{f\cos\gamma}{1-f}, \tag{6}$$

which satisfies the condition at infinity, Eq. (4). Using the inextensibility condition (1b), we now write

$$|\mathbf{r}'|^2 = 1 - |\mathbf{r}'_x|^2 = 1 - \frac{\cos^2\gamma}{(1-f)^2}. \tag{7}$$

Multiplying Eq. (5b) by $\bar{\mathbf{r}}'$, the real part leads to

$$(1-f)[|\mathbf{r}'|^2]' - 2f'|\mathbf{r}'|^2 - \lambda^2(r^2)' = 0. \tag{8}$$

As will be shown below, the fiber crosses the axis of the helix at the point of maximum tension force; we define this point to be $\xi = 0$. Furthermore, we find it convenient to define $r = |\mathbf{r}|$ for $\xi \geq 0$ and $r = -|\mathbf{r}|$ for $\xi \leq 0$.

Substituting expression (7) into Eq. (8) one obtains $f' = -\lambda^2(r^2)'/2$. This and condition (4) yield the relation

$$f = \frac{\lambda^2}{2}(1-r^2). \tag{9}$$

Substituting Eq. (9) back into Eq. (5b) and rearranging leads to

$$\mathbf{r}'' - \frac{\lambda^2}{2}[(1-r^2)\mathbf{r}']' - \lambda^2\mathbf{r} - 2i\lambda\mathbf{r}' = 0. \tag{10}$$

In solving this 2D vector equation, we choose to represent the vector $\mathbf{r}$ by means of the complex representation

$$\mathbf{r} = re^{i\phi}. \tag{11}$$

In particular, we note that in the initial geometry, ϕ is given by the linear relation $\phi = s\lambda$. Substituting Eq. (11) into Eq. (10), separating the real and imaginary parts, we obtain

$$\left[1 - \frac{\lambda^2}{2}(1-r^2)\right][r'' - (\phi')^2 r] + \lambda^2 r(r')^2 - \lambda^2 r + 2\lambda\phi' r = 0, \tag{12a}$$

$$\left[1 - \frac{\lambda^2}{2}(1-r^2)\right](\phi'' r + 2\phi' r') + \lambda^2 r^2 r'\phi' - 2\lambda r' = 0. \tag{12b}$$

Note that these equations are satisfied by the initial shape of the helix ($r = 1, \phi' = \lambda$). However, as we now show, these equations also lead to a solitary wave solution. To this end we first consider Eq. (12b) which is linear and of first order in $\psi \equiv \phi'$. Taking into account the initial helix shape as mentioned above, Eq. (12b) possesses a solution

$$\psi \equiv \phi' = \lambda\left[1 - \frac{\lambda^2}{2}(1-r^2)\right]^{-1}. \tag{13}$$

Substitution of this last result in Eq. (12a) yields a second-order equation with respect to r, namely,

$$r'' + \lambda^2 r\left[1 - \frac{\lambda^2}{2}(1-r^2)\right]^{-2} + \lambda^2 r[(r')^2 - 1]\left[1 - \frac{\lambda^2}{2}(1-r^2)\right]^{-1} = 0. \tag{14}$$

Upon setting $q = r'$ and letting $L(r) = q^2 - 1$, we obtain

$$\frac{dL}{dr} + \frac{2\lambda^2 r}{1 - (\lambda^2/2)(1-r^2)}L = -\frac{2\lambda^2 r}{[1-(\lambda^2/2)(1-r^2)]^2}, \tag{15}$$

whose solution under the condition $L(\pm 1) = -1$ is

$$L(r) = [\lambda^2(1-r^2) - 1][1 - (\lambda^2/2)(1-r^2)]^{-2}. \tag{16}$$

Note that using Eq. (16), we obtain from Eq. (6) and upon integrating Eq. (13),

$$u = (r-1)\cos\gamma, \tag{17a}$$

$$\phi = \lambda(r - 1 + s). \tag{17b}$$

We observe that $L \neq -1$ if $\lambda > 0$ and $|r| < 1$. At the point where $r = 0$, the derivative $q = r'$ has the nonzero value

$$r' = \frac{\lambda^2/2}{1 - \lambda^2/2} \qquad (r = 0), \tag{18}$$

thus indicating that the fiber crosses the x axis.

Using Eq. (16), we obtain, after simple integration, a relation between the coordinate $\xi \equiv s - \tau$ and the deformed helix radius, namely,

$$\ln\frac{1+r}{1-r} - \lambda^2 r = \lambda^2\xi. \tag{19}$$

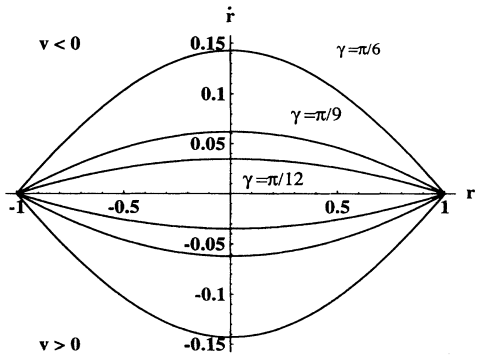

FIG. 1. Phase portrait.

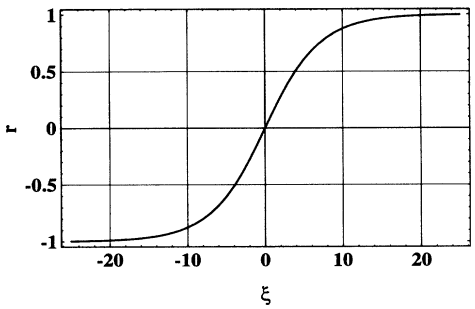

FIG. 2. Helix radius [Eq. (19)].

From this latter expression, it follows that

$$|r| \sim 1 - 2e^{-\lambda^2(1+|\xi|)} \qquad (|\xi| \to \infty); \tag{20}$$

that is, the propagating disturbance decays exponentially as $|\xi| \to \infty$.

Thus we conclude that the solution (19) corresponds to a solitary wave. It is of interest to note that the shape of the wave depends on the helix angle only and the "effective" wavelength decreases as γ increases.

Finally, we present expressions for the linear and angular momenta $\mathbf{p}$ and $\mathbf{H}$, respectively, as well as for the energy, T, of the solitary wave as functions of the helix properties, R_0, γ, and ρ, and the solitary wave parameter, v. It is worth noting that for a given helix, v is the sole parameter governing the propagation of the solitary wave. From Eq. (17a), it is evident that $\dot{u} = -u' = -r'\cos\gamma$. Then, using Eq. (2) one obtains

$$\mathbf{p} = \rho v R_0 \int_{-\infty}^{\infty} \dot{u} ds \mathbf{k}_x = -2\rho v R_0 \cos\gamma\, \mathbf{k}_x, \tag{21a}$$

$$\mathbf{H} = \rho v R_0^2 \int_{-\infty}^{\infty} r^2 \dot{\phi}\, ds \mathbf{k}_x = -\frac{2}{3}\rho v R_0^2 \sin\gamma \mathbf{k}_x. \tag{21b}$$

Noting from Eq. (17b) that $\dot{\phi} = -\lambda r'$ and using the representation, Eq. (11),

$$T = \frac{\rho v^2}{2} R_0 \int_{-\infty}^{\infty} (\dot{u}^2 + \dot{r}^2 + r^2\dot{\phi}^2)\, ds = \frac{2}{3}\rho v^2 R_0 \sin^2\gamma. \tag{22}$$

Note that as $\gamma \to 0$ the angular momentum of the wave becomes negligible compared to the linear momentum. In this case, expression (19) yields the asymptotic solution

$$r \sim \tanh\frac{\lambda^2}{2}\xi, \tag{23a}$$

$$f \sim \frac{\lambda^2}{2}\mathrm{sech}^2\left(\frac{\lambda^2}{2}\xi\right). \tag{23b}$$

The shape of the distribution of the force, Eq. (23b) coincides with that of the soliton governed by the KdV equation. However, the effective lengths of these two waves are not the same: In our case, the length depends on the helix angle, γ, while for the case of the KdV equation, it depends on the soliton velocity, v.

We present here some numerical results. In Fig. 1, the phase portrait is shown in $(r, \dot{r})$ space for several values of γ. Results shown in Figs. 2 and 3 are given for $\gamma = \pi/6$. The variation of the helix radius with ξ, based on the relation (19), is shown in Fig. 2. Using the calculated values of r, the force f, evaluated from Eq. (9), is shown as a function of $\xi = s - \tau$ in Fig. 3.

A numerical simulation, using a finite discrete system of masses connected by massless inextensible rigid links, was performed to obtain a transient wave response. (A comparison with theoretical results showed the numerical calculations to be highly accurate.) Results of these

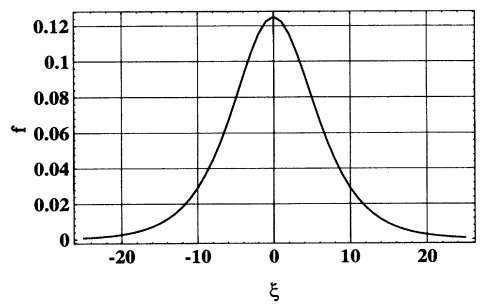

FIG. 3. Internal force [Eq. (9)].

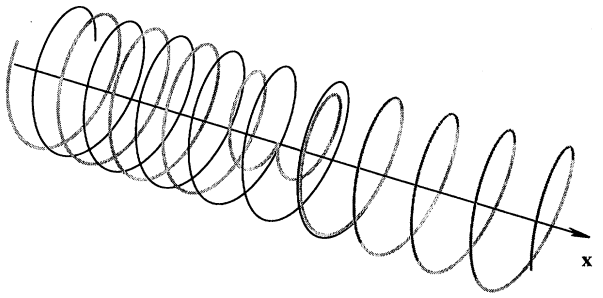

FIG. 4. Comparison of initial (black curve) and deformed (gray curve) shape of the helix.

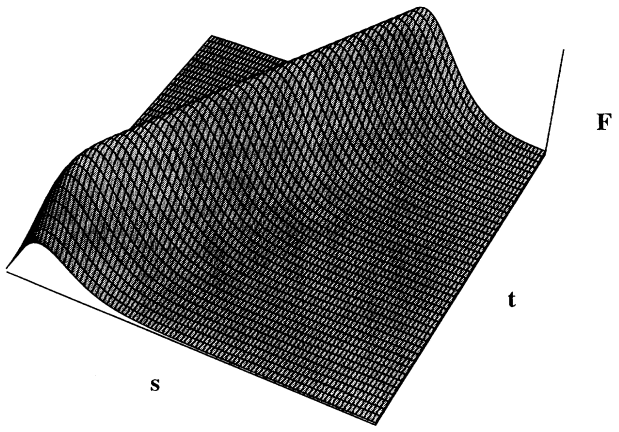

FIG. 5. Solitary wave formation in the helix under a suddenly applied force.

calculations are presented in Figs. 4 and 5. The shape of the deformed helix with respect to its initial shape is shown in Fig. 4; we note that the disturbance is limited effectively to a finite region of the helix. The spatial distribution of the force with time is presented in Fig. 5 where we observe that the wave travels as a solitary wave. Results have also been obtained for waves traveling in opposite directions. It was observed that after collision, the waves continue to travel in their respective directions but with a phase shift as is characteristic of solitary wave collisions.

This work was supported in part by the Ministry of Immigrant Absorption, Israel.

[1] O. B. Gorbacheva and L. A. Ostrovsky, Physica (Amsterdam) **8D**, 223–228 (1983).
[2] P. Rosenau, Physica (Amsterdam) **27D**, 224–234 (1987).
[3] S. Cadet, Phys. Lett. A **121**, 77–82 (1987).
[4] S. Cadet, Wave Motions **11**, 77–97 (1989).
[5] P. Rosenau and M. B. Rubin, Phys. Rev. A **31**, 3480–3482 (1985).
[6] P. Rosenau and M. B. Rubin, Physica (Amsterdam) **19D**, 433–439 (1986).
[7] M. F. Beatty and J. B. Haddow, J. Appl. Mech. **52**, 137–143 (1985).
[8] T. Shimizu, K. Sawada, and M. Wadati, J. Phys. Soc. Jpn. **50**, 1779–1802 (1981).
[9] T. Shimizu, K. Sawada, and M. Wadati, J. Phys. Soc. Jpn. **52**, 36–43 (1983).
[10] A. S. Davydov, *Theory of Molecular Excitons* (Plenum, New York, 1971).
[11] A. S. Davydov, Physica (Amsterdam) **3D**, 1–23 (1981).
[12] M. A. Davies and F. C. Moon, Chaos **3**, 93–99 (1993).
[13] A. V. Cherkaev and L. I. Slepyan, Int. J. Damage Mech. (to be published).